

Hazard prediction of coal and gas outburst based on fisher discriminant analysis

Liang Chen^{*1,3}, Enyuan Wang^{**2}, Junjun Feng², Xiaoran Wang² and Xuelong Li²

¹School of Energy & Environment Engineering, Zhongyuan University of Technology, 450007 Zhengzhou, Henan, China

²Key Laboratory of Coal Methane and Fire Control, Ministry of Education, China University of Mining and Technology, 221116 Xuzhou, Jiangsu, China

³Key Laboratory of Safety and High-efficiency Coal Mining, Ministry of Education Anhui University of Science and Technology, 232001 Huainan, Anhui, China

(Received November 19, 2015, Revised March 19, 2017, Accepted June 29, 2017)

Abstract. Coal and gas outburst is a serious dynamic disaster that occurs during coal mining and threatens the lives of coal miners. Currently, coal and gas outburst is commonly predicted using single indicator and its critical value. However, single indicator is unable to fully reflect all of the factors impacting outburst risk and has poor prediction accuracy. Therefore, a more accurate prediction method is necessary. In this work, we first analyzed on-site impacting factors and precursors of coal and gas outburst; then, we constructed a Fisher discriminant analysis (FDA) index system using the gas adsorption index of drilling cutting Δh_2 , the drilling cutting weight S , the initial velocity of gas emission from borehole q , the thickness of soft coal h , and the maximum ratio of post-blasting gas emission peak to pre-blasting gas emission B_{max} ; finally, we studied an FDA-based multiple indicators discriminant model of coal and gas outburst, and applied the discriminant model to predict coal and gas outburst. The results showed that the discriminant model has 100% prediction accuracy, even when some conventional indexes are lower than the warning criteria. The FDA method has a broad application prospects in coal and gas outburst prediction.

Keywords: coal and gas outburst; prediction; fisher discriminant analysis; indicator

1. Introduction

Coal and gas outburst often occurs in the coal-mining process and causes great damages to the coal miners on site and production safety in general. All main coal-producing countries in the world have suffered this type of dynamic disaster, with approximately one third occurring in China. The disaster is one of the major safety challenges to the coal mine industry in China (Xu *et al.* 2006, Skoczylas 2012). With the mining depth increasing and geological conditions becoming more complicated, coal and gas outburst disaster also become more and more serious. In addition, according to a statistical analysis by the Chinese National Administration of Work Safety and National Coal Mine Safety, the number of outburst mines in China increased from 647 in 2007 to

*Corresponding author, Ph.D., E-mail: chenliang851121@163.com

**Corresponding author, Professor, E-mail: weycumt@yeah.net

1,191 in 2012 and is continuously increasing by approximately 3% per year. Both the increased seriousness of coal and gas outburst disaster and the ever-increasing number of outburst mines represent significant challenges. Although the upward trend of coal and gas outburst accidents has been gradually controlled recently, the resulting casualties have not been completely eliminated. One of the important reasons for this is that coal and gas outburst become more and more complex, making it more and more difficult to predict it accurately.

Coal and gas outburst is the interactive result of stress, gas pressure, and coal's physical and mechanical properties. Therefore, a series of indicators are proposed and used to predict coal and gas outburst disaster. The indicators include the initial velocity of gas emission from boreholes, drilling cutting weight, etc. The method of using indicators' critical value has been broadly applied to determine the risk of outburst in many countries. In addition, other non-continuous forecasting methods that detect the methane concentration and V_{30} (Yang *et al.* 2010, Torano *et al.* 2012), the coal's desorption performance V_1 (Fernandez-Diaz *et al.* 2013), the gas content for gas outburst prediction (Xue *et al.* 2014) and the gas dilatation energy (Jiang *et al.* 2015, Yu *et al.* 2015) have been used to predict coal and gas outburst. In recent years, geophysical methods, such as microseismic (Ding *et al.* 2016, Liu *et al.* 2016), acoustic emission (Xiao *et al.* 2016, Wen *et al.* 2016), and electromagnetic radiation (He *et al.* 2012, Wang *et al.* 2014) methods, have developed rapidly. Use of these methods has been attempted in some coal mines.

However, the prediction of coal and gas outburst using a single indicator cannot fully reflect the risk of gas outbursts. This method is even inaccurate sometimes. Comprehensive prediction with multiple indicators can overcome the disadvantage of using a single indicator, improve the prediction accuracy and be widely applied. The methods are as follows.

A gas-measurement-tube set has been designed. Its purpose is to measure gas pressure and its variation over time as a result of nearby workings and to calculate permeability to assess the potential outburst-prone areas (Aguado and Nicieza 2007).

Well tests for permeability and stress have been performed in holes, and recovered core has been tested in a laboratory for permeability, strength and sorption properties. The test data and Monte Carlo techniques are used to evaluate the risk of outburst (Wold *et al.* 2008).

Zhang *et al.* (2009) established a comprehensive evaluation index system that includes gas content and gas pressure and is based on catastrophe theory to predict the risk of coal and gas outburst. Wen *et al.* (2016) proposed the correlation between the formation process of rockburst and the evolution of overlying strata spatial structure of the stope, criterion of rockburst occurrence, new classification, and predictive evaluation method for rockburst hazard that rockburst damage evaluation (RDE)=released energy capacity (REC)/absorbed energy capacity (AEC). Many researches have separately adopted the artificial neural network (ANN), the support vector machine (SVM) and elliptic orbit mode to predict coal and gas outburst (Zhang and Ian 2010, Chen *et al.* 2014, Li *et al.* 2015, Yang and Zhou 2015). An attribute synthetic evaluation model for predicting the risk of coal and gas outburst has also been proposed. It included six indexes, gas pressure of coal seam, the initial speed of methane diffusion, the firmness coefficient, types of the coal damage, comprehensive index of D and K (Ma *et al.* 2012). In addition, a gray target model has been established based on gray system theory to predict coal and gas outburst. The model considers four influencing factors for coal and gas outburst: gas pressure, the destructive type of coal, coal rigidity, and the initial speed of methane diffusion (Hu *et al.* 2015).

All of these prediction methods meet the need of some coal mines for outburst prediction to some extent. However, their poor accuracy and slow computing speed have limited further application. For example, although catastrophe theory and gray target model have simple

calculations, their accuracy is poor. Although ANN is highly accurate, it has slower convergence speed. For linearly separable samples, Fisher discriminant analysis (FDA) can always find a projection direction. The samples are still separable in linearity after lowering their dimension and have better reparability. The advantage is extensively applicable for type identification and classification. In other words, FDA can separate different types of samples as distantly as possible and concentrate the same type of samples as closely as possible. This property of FDA is very appropriate for the multi-index comprehensive prediction of coal and gas outburst. FDA has been successfully applied to face recognition, gene expression data classification, and so on (Huang *et al.* 2012, Moulin *et al.* 2014, Wang *et al.* 2015). This work will attempt to establish a multi-index model for the discrimination of coal and gas outburst using on-site prediction index data and FDA. The model is then applied in the field to predict coal and gas outburst.

2. Fisher discriminant analysis

The basic idea of FDA method lies in the projection of high-dimensional data points into a lower dimensional space. It makes data points more concentrated in the low-dimensional space, thereby overcoming the “curse-of-dimensionality” caused by higher dimension. The specific process includes 1) applying the principle of “maximizing the inter-type distance and minimizing the intra-type distance” to establish the discriminant function, and 2) using the established discriminant function to identify the sample type (Chen *et al.* 2009, Rahman *et al.* 2015).

2.1 FDA resolution

FDA can convert a multi-dimensional problem into a one-dimensional problem while still using a linear discriminant function to solve multiple general discriminant problems. Given a total of m known groups G_1, G_2, \dots, G_m with corresponding mean vectors and covariance matrices $\mu^{(1)}, \mu^{(2)}, \dots, \mu^{(m)}$, and $V^{(1)}, V^{(2)}, \dots, V^{(m)}$, respectively, the sample with capacity n_i extracted from group G_i is calculated as follows

$$X_{\alpha}^{(i)} = (x_{\alpha 1}^{(i)}, x_{\alpha 2}^{(i)}, \dots, x_{\alpha p}^{(i)})^T \tag{1}$$

Thus,

$$u^T X_{\alpha}^{(i)} = (u_1 x_{\alpha 1}^{(i)}, u_2 x_{\alpha 2}^{(i)}, \dots, u_p x_{\alpha p}^{(i)})^T \tag{2}$$

is the projection of $X_{\alpha}^{(i)}$ on the u -axis, where $\alpha=1, 2, \dots, n_i; i=1, 2, \dots, m$; the vector $u=(u_1, u_2, \dots, u_p)^T$ denotes one direction in the p -dimensional space; and $Y = U^T X$ is the scalar product of u and X , namely, the projection of X on the u -axis.

Let

$$\bar{X}^{(i)} = \frac{1}{n_i} \sum_{\alpha=1}^{n_i} X_{\alpha}^{(i)} \tag{3}$$

and

$$\bar{X} = \frac{1}{n} \sum_{i=1}^m \sum_{\alpha=1}^{n_i} X_{(\alpha)}^{(i)} \quad (4)$$

where $n = \sum_{i=1}^m n_i$; $\bar{X}^{(i)}$ and \bar{X} are the mean of intra-group samples and the mean of total samples, respectively. Then, the intra-group difference is calculated as follows

$$\begin{aligned} e &= \sum_{i=1}^m \sum_{\alpha=1}^{n_i} (u^T X_{(\alpha)}^{(i)} - u^T \bar{X}^{(i)})^2 = \\ &u^T \left\{ \sum_{i=1}^m \left[\sum_{\alpha=1}^{n_i} (X_{(\alpha)}^{(i)} - \bar{X}^{(i)})(X_{(\alpha)}^{(i)} - \bar{X}^{(i)})^T \right] \right\} u = \\ &u^T \left\{ \sum_{i=1}^m S_i \right\} u = u^T W u \end{aligned} \quad (5)$$

where S_i is the dispersion matrix of n_i samples in G_i , $X_{(\alpha)}^{(i)}$, ($\alpha=1, 2, \dots, n_i$). The inter-group difference is expressed as follows

$$b = \sum_{i=1}^m \sum_{\alpha=1}^{n_i} (u^T \bar{X}^{(i)} - u^T \bar{X})^2 = u^T \left[\sum_{i=1}^m (\bar{X}^{(i)} - \bar{X})(\bar{X}^{(i)} - \bar{X})^T \right] u = u^T B u \quad (6)$$

Let $\phi = \frac{b}{e} = \frac{u^T B u}{u^T W u}$. To maximize ϕ and make the solution unique, an additional condition is commonly added: $u^T W u = 1$. Under the condition $u^T W u = 1$, the problem becomes finding u to maximize $u^T B u$. For this purpose, it is necessary to apply the Lagrange multiplier method.

Set

$$F = u^T B u - \lambda(u^T W u - 1) \quad (7)$$

Differentiating Eq. (7) with respect to u and making the resultant expression equal to zero yield the following

$$\frac{\partial F}{\partial u} = 2B u - 2\lambda W u = 0 \quad (8)$$

After further arrangement, the following discriminant criterion is found

$$(W^{-1}B - \lambda I)u = 0 \quad (9)$$

This equation tells us that the parameter λ is the maximum eigenvalue of $W^{-1}B$ and u is the eigenvector corresponding to the maximum eigenvalue. Thus, one can find the discriminant function.

2.2 Verification of FDA discriminant effect

To investigate the quality of the above-mentioned criterion, it is necessary to employ the

training-sample-based backward substitution method to calculate the misjudgment rate. The training-sample-based backward substitution method uses all of the training samples $X_{\alpha}^{(i)} = (x_{\alpha 1}^{(i)}, x_{\alpha 2}^{(i)}, \dots, x_{\alpha p}^{(i)})^T$ (where $\alpha=1, 2, \dots, n_i; i=1, 2, \dots, m$) extracted from group G_i and with capacity n_i as new samples. Then, it puts them in order in the established discriminant function, and applies the established discriminant criterion to predict the risk of coal and gas outburst risk. Let n_{ij} denote the number of samples in group G_i being misjudged in group G_j and N be the total number of misjudged samples. The rate of misjudgment η estimated using the backward substitution method is calculated as follows

$$\eta = \frac{N}{n_1 + n_2 + \dots + n_m} \tag{10}$$

3. Overview of coal and gas outburst on the site

Jiulishan Coal Mine of Henan Energy Chemical Group is located in Jiaozuo City, Henan Province, China, as shown in Fig. 1. The coal mine began to build in 1970 and produce in 1983. Its design production capacity is 0.9 Mt/a. This work chose the No. 14141 working face of Jiulishan Coal Mine as the test site.

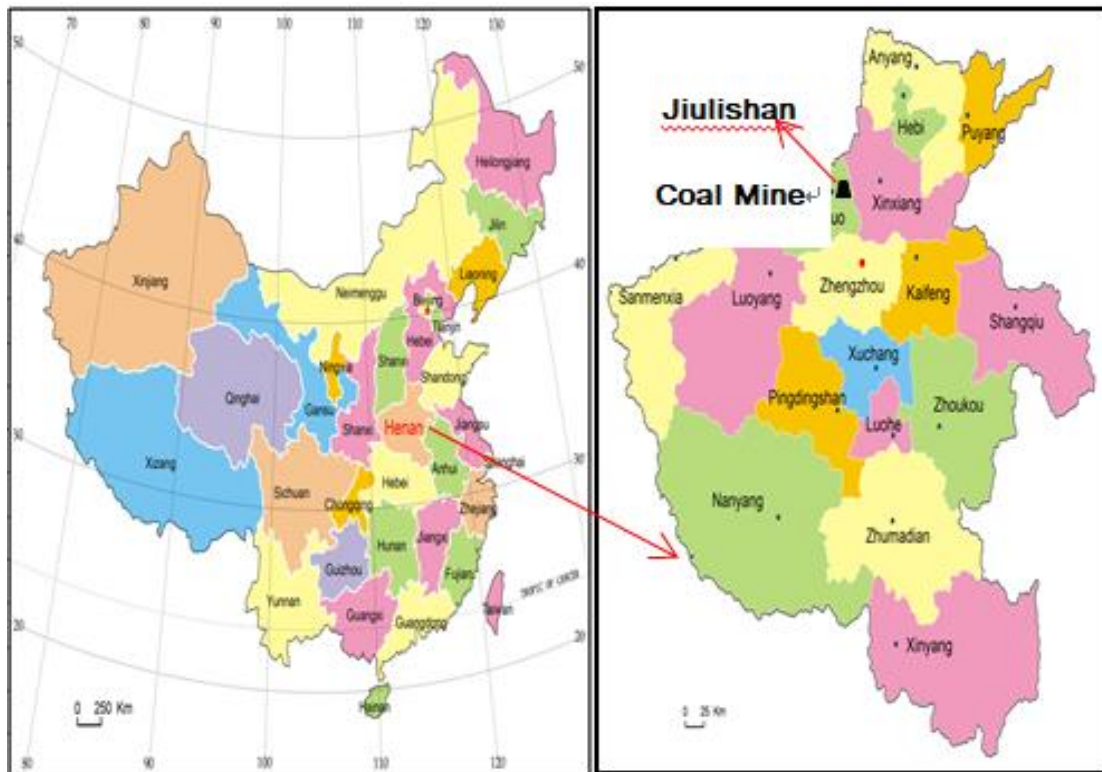


Fig. 1 Geographical location of Jiulishan Coal Mine

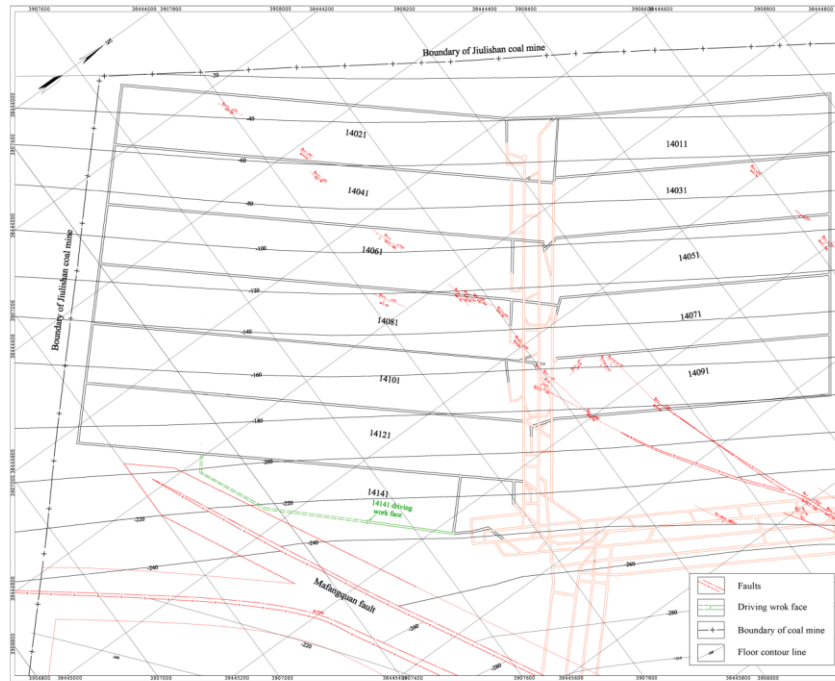


Fig. 2 No.14141 work face of Julishan Coal Mine

Stratigraphic Systems				Coal rock columnar	Thickness	Lithology				
Erathem	System	Series	Formation							
Cenozoic	Tertiary and Quaternary	Top Permian Series	Top Shihzei Formation	[Pattern]	39.71	Yellow Earth				
				[Pattern]	34.23	Red Gravel				
				[Pattern]	4.20	Coarse Conglomerate				
				[Pattern]	4.88	Red Gravel				
				[Pattern]	22.97	Red Earth				
				[Pattern]	12.88	Laterite Gravel				
				[Pattern]	15.92	Red Earth				
				[Pattern]	2.79	Sandstone				
				[Pattern]	13.08	Shale				
				Paleozoic	Permian	Lower Permian Series	Lower Shihzei Formation	[Pattern]	6.64	Sandstone
								[Pattern]	32.88	Sandy Shale
								[Pattern]	3.42	Sandstone
								[Pattern]	7.69	Sandy Shale
								[Pattern]	7.18	Sandstone
[Pattern]	29.79	Sandy Shale								
Shanxi Formation	[Pattern]	1.36	Sandstone							
	[Pattern]	24.05	Sandy Shale							
	[Pattern]	7.90	Sandstone							
	[Pattern]	3.45	Sandy Shale							
	[Pattern]	6.56	Sandstone							
[Pattern]	31.54	Sandy Shale								
[Pattern]	2.28	Sandstone								
[Pattern]	28.93	Sandy Shale								
[Pattern]	6.08	Coal of B1								
[Pattern]	11.49	Sandy Shale								

Fig. 3 Histogram of coal seam

3.1 Coalbed conditions

The No.14141 working face lies in the lowermost part of the West Wing of the 14th mining area, as shown in Fig. 2. The current mining B₁ coalbed is located at the bottom of the Shanxi Formation. Its immediate roof is mainly composed of sandy shale. The old roof is thick-bedded sandstone. Its floor is mostly sandy shale. Fig. 3 shows the comprehensive histogram of the coalbed. The roof plate is characterized by large thickness and poor gas permeability and is suitable for gas capture and storage. The gas content in the coalbed is 19.17 m³/t. The coalbed occurrence of the No.14141 working face is steady, with an average thickness of 6.08 m and inclination angle of 12°.

3.2 Analysis of the law of coal and gas outburst

The first coal and gas outburst occurred at a depth of 160 m on June 24, 1956 in Lifeng Coal Mine. This mine belongs to Jiaozuo Coal Mining Area. The B₁ coalbed in the Jiaozuo Coal Mining Area has experienced approximately 370 coal and gas outburst. Among them, 64 appeared in Jiulishan Coal Mine, as shown in Table 1. In addition, Jiulishan Coal Mine, at a burial depth of 450 m, experienced the largest coal and gas outburst, with 2,397 t of coal and 232,500 m³ of gas. The maximum amount of outburst gas per ton of coal occurring at a burial depth of 300 m is 1,778 m³/t.

Table 1 Statistics of coal and gas outburst of Jiulishan Coal Mine

Outburst time	Outburst zone	Burial depth /m	Outburst coal amount/t	Outburst gas amount/m ³	Outburst reason
1980.9.13	1231 air-distributing hole	160	3	—	roadway support
1981.3.15	11211 air-distributing hole	190	82	5012	blasting
1984.11.9	11061 haulageway crosscut	236	60	8889	blasting
1985.4.23	11041 haulageway crosscut 2	211	39	2439	blasting
1985.4.27	11041 haulageway crosscut 2	211	61	4525	blasting
1985.7.17	11041 haulageway crosscut 2	208	19	1801	blasting
1985.9.5	11041 haulageway crosscut 2	207	40	4041	blasting
1985.9.12	11041 haulageway crosscut 3	207	13	5448	blasting
1985.11.23	11061 haulageway westward	235	24	5291	blasting
1985.11.26	11061 haulageway westward	235	94	12793	blasting
1986.1.2	11061 haulageway	235	28	2293	blasting
1986.1.27	11061 haulageway	235	15	1630	blasting
1986.2.3	11051 face	234	0	1555	machine mining
1986.10.25	11051 face	234	53	5124	machine mining

Table 1 Continued

Outburst time	Outburst zone	Burial depth /m	Outburst coal amount/t	Outburst gas amount/m ³	Outburst reason
1986.11.3	11051 face	234	30	44805	machine mining
1986.11.25	11091 connecting roadway	304	8.2	5441	drilling
1987.7.8	11091 connecting roadway	305	33	2483	blasting
1987.7.21	11091 connecting roadway	295	16	2072	blasting
1987.9.4	11051 face	236	72.5	1872	machine mining
1987.9.11	11051 face	231	34	741	machine mining
1987.9.21	11051 face	230	123.5	3446	machine mining
1987.12.7	11051 face	230	11.3	513	machine mining
1988.12.4	12051 excavating roadway	230	20	2205	blasting
1989.3.17	11091 haulageway	300	318	41807	blasting
1989.7.23	11091 haulageway	300	170	8551	blasting
1990.3.5	11091 haulageway	300	4.5	8000	blasting
1991.1.7	11091 haulageway	291	540	58490	blasting
1991.9.10	11071 face	240	140	15224	blasting
1991.9.14	11071 face	240	129	12855	machine mining
1992.2.16	11071 face	256	13	2601	blasting
1995.4.13	13081 haulageway	280	68	9624	blasting
1995.10.27	13091 haulageway	–	3	–	machine mining
1995.10.30	13091 haulageway	–	3	–	machine mining
1996.11.25	11091 connecting roadway	304	5.2	5441	drilling
2000.11.17	15011 haulageway	397	315	34574	blasting
2001.11.4	15011 haulageway	–	96	9800	blasting
2003.12.30	14081face	206	75	7015	machine mining
2004.12.16	15061 excavating roadway	412	570	55452	hydraulic slotting
2005.4.22	15061 excavating roadway	412	30	5840	blasting
2005.6.10	15061 excavating roadway	408	308	2588	blasting
2005.8.23	15051 section roadway	450	2397	232500	blasting
2006.3.6	14121 haulageway	302	1072	134000	blasting
2006.8.23	14121 haulageway	302	925	116000	hydraulic slotting
2006.12..9	15041 haulageway	401	43	14198	blasting
2007.4.26	15041 haulageway	395	87	2244	blasting
2007.5.26	15031 haulageway	413	124	16876	hydraulic slotting
2007.6.18	15041 excavating roadway	388	20	4221	blasting
2007.9.16	15031 haulageway	413	214	28300	hydraulic slotting
2007.9.28	15041 excavating roadway	389	135	10200	blasting
2007.11.24	24 excavating roadway	333	120	14000	hydraulic slotting
2008.1.2	Return airway east main roadway	308	180	22000	hydraulic slotting

Table 1 Continued

Outburst time	Outburst zone	Burial depth /m	Outburst coal amount/t	Outburst gas amount/m ³	Outburst reason
2008.2.18	15051 haulageway	439	475	22800	hydraulic slotting
2008.3.10	15081 section roadway	461	149	20700	hydraulic slotting
2008.7.30	15081 section roadway	461	87	12080	blasting
2008.8.16	15031 haulageway	413	45	5895	hydraulic slotting
2008.8.17	15051 haulageway	439	50	6550	blasting
2008.9.21	15031 haulageway	413	92	11960	blasting
2008.10.20	15031 haulageway	413	64	6976	blasting
2008.10.23	15031 haulageway	413	110	11925	hydraulic slotting
2009.3.13	24021 haulageway. external section	359	112	11925	blasting
2009.3.27	24 raise	372	63	7935	blasting
2009.4.3	15071 haulageway	439	189	16500	hydraulic slotting
2009.7.24	24021 external section of haulageway	344	103	22000	hydraulic slotting
2009.8.1	24020 external section of haulageway	344	238	35350	hydraulic slotting

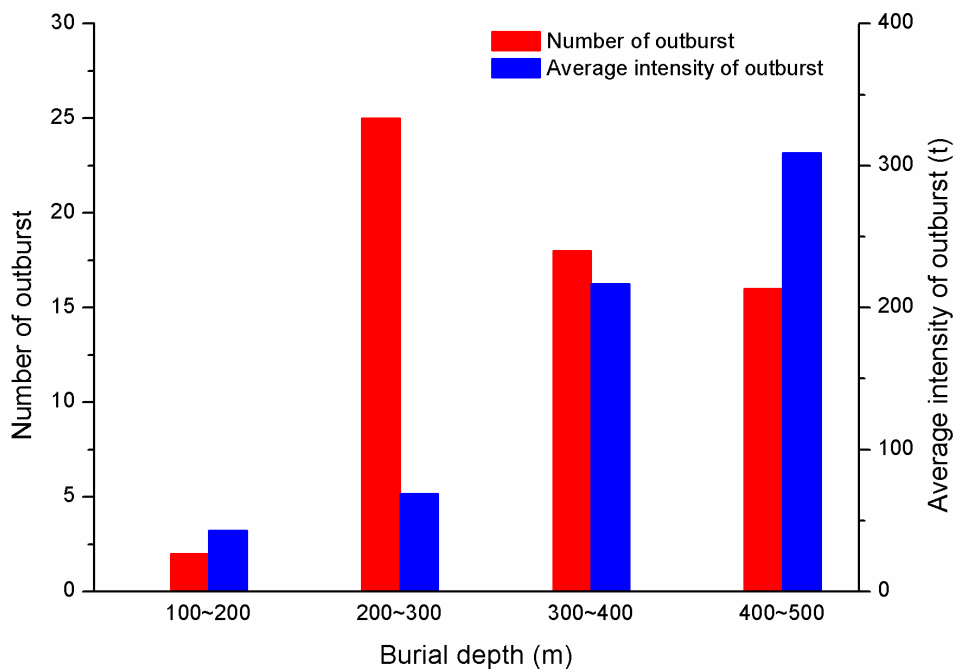


Fig. 4 Number of coal and gas outburst and average intensity of outburst gas at different mining depths

Fig. 4 shows the relationships between both the number of coal and gas outburst and the average intensity and the burial depth. It is clear from the figure that as the burial depth increases,

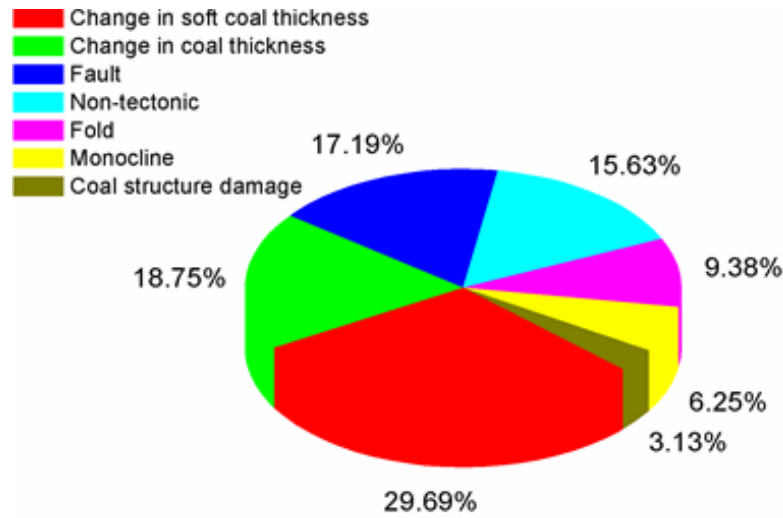


Fig. 5 Effects of geological structures, soft coal, and others on coal and gas outburst

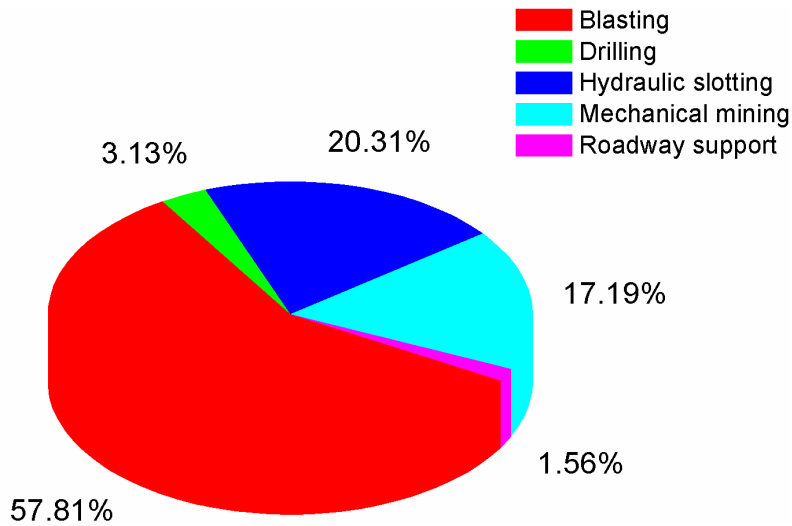


Fig. 6 Distribution of coal and gas outburst induced by different disturbances

the number of outbursts does not show a continuously increasing trend. The numbers are 25 times at 200-300 m, 18 times at 300-400 m, and 16 times at 400-500 m. However, this does not indicate that the risk of outbursts declines as the burial depth increases. Rather, this trend is related to improvements in coal and gas outburst prevention, control techniques, management measures, and the mining area layout in recent years (Wang *et al.* 2014, Zhou *et al.* 2016).

Fig. 4 also shows that as the burial depth increases, the average intensity of outbursts apparently increases to 309 tons at 400-500 m. As the burial depth increases, the intensity of coal and gas outburst also increases; thus, coal and gas outburst disaster prevention and control tasks have become more and more important. The No.14141 face has a burial depth of approximately

320 m; obviously, it is at a higher risk of coal and gas outburst.

3.3 Impacting factors for coal and gas outburst

Geology, soft coal, coal thickness, etc. are the important factors for coal and gas outburst. Fig. 5 shows the statistics for geological conditions, soft coal and other factors of outburst sites in Jiulishan. Based on the figure, it is clear that among these factors, changes in the thickness of soft coal seams have the greatest effect on outbursts (inducing 19 outbursts), accounting for 29.69% of the total, followed by the changes in coal thickness (12 outbursts), accounting for 18.75%, and faults (11 outbursts), accounting for 17.19%. Non-structure and fold ranked fourth and fifth (10 and 6 outbursts), accounting for 15.63% and 9.38%, respectively. Monoclinical structure and coal structural damage had minimal impacts on the number of outbursts (4 and 2 outbursts), accounting for 6.25% and 3.13% of the total, respectively.

In addition, most outbursts were related to exterior disturbances. Fig. 6 shows the operational causes of outbursts. Fig. 6 shows that blasting is a major factor of outbursts, followed by hydraulic slotting, machine mining, drilling and roadway support. They induced 37, 13, 11, 2 and 1 outburst, accounting for 57.81%, 20.31%, 17.19%, 3.13% and 1.56%, respectively.

Overall, changes in soft coal thickness are the main internal factor of coal and gas outburst, whereas blasting is the major induction factor. Therefore, changes in soft coal thickness can be used to predict outburst risk, and it is necessary to adequately prepare for the prevention of coal and gas outburst before blasting.

3.4 Precursors of coal and gas outburst

Various different audible or silent precursors often occur prior to the most coal and gas outburst accidents. These include large great coal gun, coal bump from the wall, ribs spalling, great increase in flying dust, abnormal gas emission, anti-drilling. All of these have occurred at Jiulishan Coal Mine. Among these precursors, the abnormal increase and rapid fluctuation of gas emission are the typical precursors of coal and gas outburst (Saghafi *et al.* 2008). Thus, gas emission can be used to predict coal and gas outburst.

4. System of forecast indicators

According to FDA, the first is to determine the indicators used for the prediction of coal and gas outburst risk. Indicators at the working face that are commonly used in China include conventional borehole indicators and auxiliary indicators. The former mainly includes the initial velocity of gas emission from drilling boreholes q , drilling cutting weight S , the indexes of desorption from drilling cutting K_1 and Δh_2 . The latter includes dynamic changes in gas emission, the gas content, the electromagnetic radiation intensity from coal rock at the working face, and geological conditions in the front of the face analyzed by drilling exploration or other means.

The main indicators used to predict coal and gas outburst risk in Jiulishan Coal Mine are the drilling cutting gas desorption index Δh_2 , drilling cutting weight S , and initial speed of borehole gas emission q . The above analysis of coal and gas outburst in Jiulishan Coal Mine indicated that changes in soft coal thickness are the main internal factor. Abnormal gas emission is the precursor of outburst. Therefore, changes in soft coal thickness and gas emission should be chosen as the

prediction indicators. Their physical meanings are next briefly introduced.

4.1 Borehole indicators

To use the borehole indicator method for the prediction of outburst risk at the face, at least 3 boreholes of 42 mm in diameter and 8-10 m in depth are drilled from the face to the proper position deep into the coalbed. The three boreholes should be distributed in the soft subbed as far as possible, one in the middle of the face and parallel to the driving direction and the orifices of the other two at a position 0.5 m away from the two ribs of the roadway and their hole-ending points at a positions 2-4 m outside the outlines on both sides of the roadway. To determine the drilling cutting weight S , drilling cutting of 1-3 mm in size were collected at the orifice of each borehole drilling 1 m into the coalbed. To detect the gas desorption index Δh_2 , drill cuttings 1-3 mm in size were collected at the orifice of each borehole drilling 2 m into the coalbed. The initial velocity of gas emissions from borehole q was measured within 2 minute after drilling was stopped.

1) Index of gas desorption from drill cuttings Δh_2 .

The index of gas desorption from drill cuttings comprehensively reflects the coal's degree of damage and gas pressure, the two key factors related to outburst risk. The larger the index is, the more serious the coal damage, the larger the pressure of gas, and the larger the coal and gas outburst risk is. The critical Δh_2 value for outburst risk is 200 Pa.

2) Drilling cutting weight S

The drilling cutting weight considers the main factors determining the risk of outbursts, i.e., the stress, gas pressure, and the coal's physical and mechanical properties. The larger the index is, the larger the risk is of coal and gas outburst. The critical S value for outburst risk is 6 kg/m.

3) Initial velocity of gas emission from borehole q

The initial velocity of gas emission from borehole comprehensively reflects the gas pressure, coal's physical and mechanical properties, and the gas permeability of coal. The higher the index is, the greater the risk of coal and gas outburst. The critical q value for outburst risk is 5 L/min.

4.2 Soft coal

Soft coal suffers from severe geological structural damage and is characterized by low mechanical strength, poor gas permeability and a high initial velocity of gas emission. Soft coal was present in all of the sites where coal and gas outburst occurred (Cao *et al.* 2001) and is a criterion for the occurrence of coal and gas outburst. Protodyakonov's coefficient for coal f describes the ability of coal to resist coal and gas outburst. The softer the coal is, the smaller the coefficient is. Protodyakonov's coefficient f of the No.14141 face of Jiulishan Coal Mine is 0.2-0.3, far below the national standard of 0.5. Therefore, the coalbed is prone to outbursts. In addition, the occurrence of outbursts at Jiulishan Coal Mine was mostly the result of soft coal. The thicker the soft coal is, the easier it is for the coal to suffer from damage and the larger the outburst risk is. The thickness of soft coal h as a prediction index reflects the outbursts risk of the face and can be obtained from on-site measurements.

4.3 Gas emission

The wide application of a gas monitoring system has made it very convenient to use gas emission anomaly to predict coal and gas outburst. On the premise of both relatively stable air

flow and correct arrangement of gas sensors, the pre-blasting concentration of gas C measured by the gas sensor reflects the normal gas desorption capacity of a coalbed, whereas the post-blasting concentration peak of gas P reflects the post-blasting disturbance desorption capacity, as well as the gas-supplying capacity of coalbed pores and cracks and other factors impacting outbursts. An abnormal increase in the post-blasting gas concentration indicates an abnormal enlargement in factors affecting outbursts in the region. In other words, the risk of outbursts occurring in this region increases. Thus, the maximal ratio of the post-blasting gas emission peak P to the pre-blasting gas concentration C , i.e., $B_{\max}=P/C$, can be used to reflect the risk of coal and gas outburst (Li and Zhou 2012). The concentration of gas can be directly obtained through the gas monitoring system.

5. FDA-based discriminant model and verification

Based on the measured data from multiple-groups and the basic concept of FDA, this work established the FDA function of coal and gas outburst. The accuracy of the FDA model is tested using the backward substitution method. This model can be applied in the field if it is accurate.

5.1 FDA model for coal and gas outburst

Based on the drilling cutting gas desorption index Δh_2 , the drilling cutting weight S , the initial velocity of borehole gas emission q , the thickness of soft coal h , and the maximal ratio between the post-blasting gas emission peak and pre-blasting gas concentration B_{\max} , of 58 groups of measurements obtained from the No.14141 working face of Jiulishan Coal Mine, we established an FDA model. Table 2 lists the 58 groups of data obtained from the No.14141 working face of Jiulishan Coal Mine.

Table 2 Outburst risk prediction indexes and backward substitution check-up of discriminant results

Group	Gas adsorption index of drilling cutting $\Delta h_2/\text{Pa}$	Drilling cutting weight $S/\text{kg}\cdot\text{m}^{-1}$	Initial velocity of gas emission from borehole $q/\text{L}\cdot\text{min}^{-1}$	Soft coal thickness h/m	Ratio of post-blasting gas emission peak to pre-blasting gas emission B_{\max}	Actual risk	Discriminant function value	Square of distance from non-outburst centroid	Square of distance from outburst centroid	Forecast risk
1	180	2.4	2	0.5	1.22	N	-0.53	0.09	32.95	N
2	180	2.6	1.5	1.1	7.25	N	-0.01	0.68	27.25	N
3	180	2.6	3.5	0.6	5.26	N	1.04	3.51	17.40	N
4	160	2.4	1.5	1.4	6.43	N	-1.88	1.10	50.33	N
5	180	2.8	2	1	4.50	N	0.70	2.36	20.34	N
6*	180	3.8	3.5	0.6	6.19	Y	6.17	49.06	0.92	Y

Table 2 Continued

Group	Gas adsorption index of drilling cutting $\Delta h_2/\text{Pa}$	Drilling cutting weight $S/\text{kg}\cdot\text{m}^{-1}$	Initial velocity of gas emission from borehole $q/\text{L}\cdot\text{min}^{-1}$	Soft coal thickness h/m	Ratio of post-blasting gas emission peak to pre-blasting gas emission B_{\max}	Actual risk	Discriminant function value	Square of distance from non-outburst centroid	Square of distance from outburst centroid	Forecast risk
7	160	2.4	1.5	1.1	4.19	N	-1.66	0.69	47.26	N
8	180	2.4	3.5	0.8	3.92	N	-0.36	0.22	31.08	N
9	160	2.4	1.5	0.7	1.63	N	-1.31	0.22	42.49	N
10	160	2.4	1.5	0.7	2.46	N	-1.18	0.12	40.88	N
11*	180	3.6	3.5	0.6	5.98	Y	5.31	37.71	0.01	Y
12	160	2.4	1.5	0.6	3.12	N	-0.90	0.00	37.33	N
13	120	2.4	1.5	0.6	1.82	N	-1.82	0.97	49.46	N
14	100	2.6	1.5	0.7	1.44	N	-1.60	0.58	46.34	N
15	140	2.4	2	0.5	1.91	N	-1.15	0.10	40.51	N
16	360	3.2	2	0.6	2.82	Y	6.13	48.51	0.84	Y
17	120	2.4	1.5	0.7	1.65	N	-2.03	1.43	52.47	N
18	140	2.4	1.5	0.5	2.61	N	-1.15	0.10	40.52	N
19	140	2.6	1.5	0.6	2.44	N	-0.53	0.09	32.99	N
20	180	2.4	2.5	1.2	2.58	N	-1.51	0.46	45.24	N
21	160	2.4	1.5	1	2.99	N	-1.66	0.68	47.19	N
22	180	2.6	1.5	0.9	2.78	N	-0.31	0.28	30.47	N
23	140	2.4	1.5	0.9	3.71	N	-1.73	0.80	48.16	N
24	520	3	2.6	0.6	5.23	Y	8.70	90.89	12.16	Y
25	180	2.8	3.5	1.3	2.45	N	0.16	0.98	25.56	N
26	180	2.4	1.5	1.1	1.77	N	-1.66	0.68	47.24	N
27	80	2.4	1.5	0.6	3.55	N	-2.29	2.12	56.29	N
28	180	2.4	2	0.5	1.74	N	-0.45	0.15	32.06	N
29	180	2.6	2.5	1.1	1.45	N	-0.67	0.03	34.56	N
30	180	2.6	3	0.8	8.00	N	0.98	3.27	17.95	N
31	180	2.4	1.5	1.1	4.13	N	-1.31	0.22	42.50	N
32	180	2.6	2	0.8	4.69	N	0.27	1.22	24.43	N
33*	180	3.4	2	0.5	9.51	Y	4.87	32.57	0.11	Y
34	180	2.4	2.5	0.6	7.17	N	0.28	1.25	24.29	N
35	140	2.6	1.5	0.5	4.36	N	-0.06	0.60	27.78	N
36	160	2.4	1.5	0.4	5.17	N	-0.22	0.38	29.52	N
37	120	2.4	1.5	0.4	3.42	N	-1.21	0.14	41.26	N

Table 2 Continued

Group	Gas adsorption index of drilling cutting $\Delta h_2/\text{Pa}$	Drilling cutting weight $S/\text{kg}\cdot\text{m}^{-1}$	Initial velocity of gas emission from borehole $q/\text{L}\cdot\text{min}^{-1}$	Soft coal thickness h/m	Ratio of post-blasting gas emission peak to pre-blasting gas emission B_{\max}	Actual risk	Discriminant function value	Square of distance from non-outburst centroid	Square of distance from outburst centroid	Forecast risk
38	100	2.4	1.5	0.4	4.82	N	-1.37	0.28	43.26	N
39	120	2.4	1.5	0.8	4.67	N	-1.76	0.87	48.67	N
40	120	2.4	1.5	0.6	4.78	N	-1.38	0.30	43.42	N
41	180	2.6	2.5	0.8	2.86	N	0.10	0.87	26.14	N
42	180	2.4	2	1	1.96	N	-1.34	0.26	42.97	N
43	140	2.4	2.5	0.6	3.87	N	-0.94	0.01	37.83	N
44	340	3	3.5	1.1	5.95	Y	4.79	31.68	0.17	Y
45	160	2.4	1.5	0.5	2.22	N	-0.85	0.00	36.72	N
46	300	2.4	3.4	0.5	5.6	N	2.61	11.85	6.78	Y
47	120	2.4	3.5	0.4	1.89	N	-1.02	0.03	38.83	N
48	180	2.4	2.5	0.4	3.05	N	0.04	0.76	26.79	N
49	120	2.6	2.5	0.5	5.33	N	-0.07	0.59	27.87	N
50	120	2.4	2.5	0.3	2.73	N	-0.92	0.01	37.58	N
51	120	2.4	3	0.5	2.41	N	-1.23	0.16	41.51	N
52	180	2.4	3.5	0.6	1.36	N	-0.38	0.21	31.23	N
53	180	2.4	2	0.7	2.52	N	-0.70	0.02	34.98	N
54	160	2.4	2	0.8	3.57	N	-1.10	0.07	39.79	N
55	160	2.4	2	0.7	3.25	N	-0.96	0.02	38.07	N
56	300	2.6	3.5	0.6	4.51	Y	3.11	15.57	4.41	Y
57	180	2.4	1.5	0.6	3.19	N	-0.52	0.10	32.89	N
58	180	2	2.5	0.4	3.60	N	-1.54	0.50	45.65	N

“*” denotes the gas spurting from borehole

“Y” denotes outburst risk, “N” denotes non-outburst risk

Table 3 Structural matrix

Forecast indicators	Coefficient
Drilling cutting weight S	0.54
Gas adsorption index of drilling cutting Δh_2	0.472
Initial velocity of gas emission from borehole q	0.24
Ratio of post-blasting gas emission peak to pre-blasting gas emission B_{\max}	0.234
Soft coal thickness h	-0.052

Table 4 Forecast results

Group	Gas adsorption index of drilling cutting $\Delta h_2/\text{Pa}$	Drilling cutting weight $S/\text{kg}\cdot\text{m}^{-1}$	Initial velocity of gas emission from borehole $q/\text{L}\cdot\text{min}^{-1}$	Soft coal thickness h/m	Ratio of post-blasting gas emission peak to pre-blasting gas emission concentration B_{\max}	Actual risk	Discriminant function value	Square of distance from non-outburst centroid	Square of distance from outburst centroid	Forecast risk
1	160	2.4	2	0.9	1.40	N	-1.61	0.59	46.48	N
2	180	2.4	2	0.9	1.54	N	-1.22	0.15	41.37	N
3	100	2.4	1.5	0.7	1.45	N	-2.42	2.53	58.32	N
4	180	2.4	2.5	0.8	6.71	N	-0.15	0.46	28.80	N
5	180	2.4	4	0.8	2.43	N	-0.48	0.12	32.41	N
6	380	2.4	3.5	0	2.03	Y	4.48	28.20	0.54	Y
7	340	2.6	4.5	1.1	4.32	Y	3.10	15.46	4.47	Y
8	180	2.6	4	1.1	6.97	N	0.48	1.72	22.43	N
9	180	2.6	1.5	1.3	4.14	N	-0.84	0.00	36.67	N
10	180	2.4	3.5	1.1	8.88	N	-0.17	0.43	29.02	N
11*	160	3.6	3.7	1.6	5.40	Y	3.05	15.07	4.68	Y
12	160	2.6	1.5	1.2	6.20	N	-0.71	0.01	35.12	N
13	360	2.4	4	0.8	1.62	Y	2.68	12.31	6.44	Y
14	60	2.4	1.5	0.5	2.13	N	-2.68	3.41	62.31	N
15*	180	3.5	4	1.2	6.19	Y	3.92	22.58	1.68	Y

“*” denotes the gas spurting from borehole

“Y” denotes outburst risk, “N” denotes non-outburst risk

The risk of coal and gas outburst is estimated based on whether the borehole index exceeds its critical value or whether dynamic phenomena, such as borehole spurting, occur. Hereafter, the presence of an outburst risk is defined as “Y”, whereas no outburst risk is defined as “N”. Table 3 lists the correlation data between the standardized discriminant variables and their function, namely, the structure matrix. According to Table 3, the structure matrix clearly shows that factors impacting the discriminant function in a descending order is the drilling cutting weight S , the drilling cutting gas desorption index Δh_2 , the initial velocity of gas emission from the borehole q , the max ratio of the post-blasting gas emission peak to the pre-blasting gas emission concentration B_{\max} , and the soft stratum thickness h .

The established discriminant function is expressed as follows

$$V = 0.018 * \Delta h_2 + 4.159 * S + 0.211 * q - 1.85 * h + 0.015 * B_{\max} - 13.466 \quad (11)$$

where V denotes the value of the discriminant function. The centroids of the non-outburst and outburst category groups are -0.834 and 5.212, respectively.

The position of each group category is calculated according to the discriminant function. Then, we calculate their distances from the centroids of the non-outburst and outburst category groups.

In this way, we obtain the outburst or non-outburst categorization.

Adopting the backward substitution method to check the 58 groups of data yielded a prediction accuracy of 100%, as shown in Table 2. The findings reveal that the discriminant ability of the established discriminant function analysis model is very stable and accurate.

5.2 FDA model for prediction

Table 4 shows the forecast results using the above-established discriminant model to predict the risk of 15 groups of newly measured data. There is risk of outburst when the borehole indexes are higher than their critical values or dynamic phenomena, such as gas spurts from boreholes, occur.

It is clear from Table 4 that in these 15 groups of data, 5 groups were predicted to have an outburst risk. Among them, the drilling cutting gas desorption index Δh_2 of groups 6, 7, and 13 was 380 Pa, 340 Pa and 360 Pa, respectively. All of them exceeded the corresponding critical value.

Meanwhile, although the Δh_2 of groups 11 and 15 were 160 Pa and 180 Pa, respectively, both less than the critical value of 200 Pa, gas spurts from the borehole occurred. These are examples of gas outburst hazards with conventional indexes lower than the warning criteria.

In both situations, the FDA model provides accurate predictions, indicating that using the FDA model to predict coal and gas outburst is very accurate, even with conventional indexes lower than the warning criteria.

In addition, Table 4 shows that when the index is below its critical value and no outburst dynamic phenomena are present, the prediction made by the established FDA model is also correct, without prediction failed.

Overall, the FDA model accurately predicted coal and gas outburst with 100% accuracy; thus, it is a good method for coal and gas outburst prediction. The method utilizes the established comprehensive relationship between outburst risk and different forecast indicators to predict the outburst risk. The critical values of the model or single prediction indexes do not need to be determined. This model is characterized by high accuracy, a fast calculation speed, and a simple algorithm. And it can be broadly applied for the prediction of coal and gas outburst risk.

6. Conclusions

The accurate prediction of coal and gas outburst is significant for coal mines. With the increase of the mining depth, coal and gas outburst has become more complex and its precise prediction has become more difficult. Therefore, a new prediction method should be developed.

(1) According to the analytical results of coal and gas outburst on site and in drilling borehole indexes, we established the FDA prediction index system. The index system consists of the drilling cuttings gas desorption index, Δh_2 , the drilling cutting weight S , the initial velocity of borehole gas emission, q , the soft coal thickness h , and the maximal ratio of the post-blasting gas emission peak to pre-blasting gas concentration, B_{\max} .

(2) Fisher discriminant analysis (FDA) is introduced as the prediction method, and a coal and gas outburst FDA model is constructed. The validation results indicated that the model has zero misjudgments and is very stable and accurate.

(3) We applied the model to predict the outburst risk of Jiulishan Coal Mine. The results showed that the method could accurately predict coal and gas outburst with no incorrect

predictions, even for low-index outburst dynamic occurrences. That is, its prediction accuracy is 100%. The FDA method does not need to determine the critical values of single prediction indexes.

The method accurately predicted coal and gas outburst in Jiulishan Coal Mine and can be spread to coal mines with geological conditions similar to Jiulishan Coal Mine.

Acknowledgments

This work is supported by the National Science Foundation of China (No. 51604311), the Applied Research Project of Key Research Program of Henan Universities (No. 18A440006), the Technology Development Program of Henan Coal Mine Safety (No. HN17-62), and the Open Research Program of Key Laboratory of Safety and High-Efficiency Coal Mining, Ministry of Education (No. JYBSYS2017106).

References

- Cao, Y., He, D. and Glick, D.C. (2001), "Coal and gas outburst in footwalls of reverse faults", *J. Coal Geol.*, **48**(1), 47-63.
- Chen, H., Li, X., Liu, A. and Peng, S. (2009), "Identifying of mine water inrush sources by Fisher discriminant analysis method", *J. Centr. South U.*, **40**, 1114-1120.
- Chen, S., Liu, J. and Chen, L. (2014), "The coal and gas outburst prediction model research based on SVM", *J. Earth Sci. Eng.*, **7**, 616-623.
- Díaz Aguado, M.B. and González Nicieza, C. (2007), "Control and prevention of gas outbursts in coal mines, Riosa-Olloniego coalfield, Spain", *J. Coal Geol.*, **69**(4), 253-266.
- Ding, Y., Dou, L., Cai, W., Chen, J., Kong, Y., Su, Z. and Li, Z. (2016), "Signal characteristics of coal and rock dynamics with micro-seismic monitoring technique", *J. Min. Sci. Technol.*, **26**, 683-690.
- Fernandez-Diaz, J.J., Gonzalez-Nicieza, C., Alvarez-Fernandez, M.I. and Lopez-Gayarre, F. (2013), "Analysis of gas-dynamic phenomenon in underground coal mines in the central basin of Asturias (Spain)", *Eng. Fail. Anal.*, **34**, 464-477.
- He, X., Nie, B., Chen, W., Wang, E., Dou, L., Wang, Y., Liu, M. and Mitrie, H. (2012), "Research progress on electromagnetic radiation in gas-containing coal and rock fracture and its applications", *Safety Sci.*, **50**(4), 728-735.
- Hu, Q., Peng, S., Xu, J., Zhang, L. and Liu, D. (2015), "Application of gray target models in the prediction of coal and gas outburst: the case of jinzhushan coal mine in China", *J. Safety Secur. Eng.*, **5**(2), 142-149.
- Huang, H., Li, J. and Liu, J. (2012), "Gene expression data classification based on improved semi-supervised local Fisher discriminant analysis", *Exp. Syst. Appl.*, **39**(3), 2314-2320.
- Jiang, C., Xu, L., Li, X., Tang, J., Chen, Y., Tian, S. and Liu, H. (2015), "Identification model and indicator of outburst-prone coal seams", *Rock Mech. Rock Eng.*, **48**(1), 409-415.
- Li, C., Liu, Y. and Zhang, H. (2015), "An improved coal and gas outburst prediction algorithm based on BP neural network", *J. Contr. Autom.*, **8**(6), 169-176.
- Li, X. and Zhou, W. (2012), "The risk forecast of coal and gas outburst on blasting-working face by the method of gas peak-to-valley ratio", *J. Chin. Coal Soc.*, **37**(1), 104-108.
- Liu, C., Li, S., Xue, J. and Yu, G. (2016), "Identification method of high fractured body for overlying strata in goaf based on microseismic monitoring technology", *J. Chin. U. Min. Technol.*, **45**(4), 709-716.
- Ma, Y., Wang, E., Liu, Z., Chen, P. and Shi, X. (2012), "Attribute synthetic evaluation model for predicting risk of coal and gas outburst", *J. Min. Safety Eng.*, **29**(3), 416-420.
- Moulin, C., LARGERON, C., DUCOTTET, C., GÉRY, M. and BARAT, C. (2014), "Fisher linear discriminant analysis

- for text-image combination in multimedia information retrieval”, *Patt. Recogn.*, **47**(1), 260-269.
- Rahman, M., Pk, M. and Uddin, M. (2015), “Optimum threshold parameter estimation of bidimensional empirical mode decomposition using fisher discriminant analysis for speckle noise reduction”, *Arab J. Info. Technol.*, **12**(5), 456-464.
- Skoczylas, N. (2012), “Laboratory study of the phenomenon of methane and coal outburst”, *J. Rock. Mech. Min. Sci.*, **55**, 102-107.
- Toraño, J., Torno, S., Alvarez, E. and Riesgo, P. (2012), “Application of outburst risk indices in the underground coal mines by sublevel caving”, *J. Rock. Mech. Min. Sci.*, **50**, 94-101.
- Wang, E., Li, Z., He, X. and Chen, L. (2014), “Application and pre-warning technology of coal and gas outburst by electromagnetic adiation”, *Coal Sci. Technol.*, **42**(6), 53-57.
- Wang, Z., Ruan, Q. and An, G. (2015), “Face recognition using double sparse local fisher discriminant analysis”, *Math. Prob. Eng.*, 1-9.
- Wen, Z., Wang, X., Lin, Q., Lin, G., Chen, S. and Jiang, Y. (2016), “Simulation analysis on the strength and acoustic emission of jointed rock mass”, *Tehnički Vjesnik-Tech. Gazette*, **23**(5), 1277-1284.
- Wen, Z., Wang, X., Tan, Y., Zhang, H. and Huang, W. (2016), “A study of rockburst hazard evaluation method in coal mine”, *Shock Vibr.*, 1-9.
- Wold, M.B., Connell, L.D. and Choi, S.K. (2008), “The role of spatial variability in coal seam parameters on gas outburst behaviour during coal mining”, *J. Coal Geol.*, **75**(1), 1-14.
- Xiao, F., Liu, G., Zhang, Z., Shen, Z., Zhang, F. and Wang, Y. (2016), “Acoustic emission characteristics and stress release rate of coal samples in different dynamic destruction time”, *J. Min. Sci. Technol.*, **26**(6), 981-988.
- Xu, T., Tang, C.A., Yang, T.H., Zhu, W.C. and Liu, J. (2006), “Numerical investigation of coal and gas outburst in underground collieries”, *J. Rock. Mech. Min. Sci.*, **43**(6), 905-919.
- Xue, S., Yuan, L., Xie, J. and Wang, Y. (2014), “Advances in gas content based on outburst control technology in Huainan, China”, *J. Min. Sci. Technol.*, **24**(3), 385-389.
- Yang, S., Tang, J., Zhao, S. and Hua, F. (2010), “Early warning on coal and gas outburst with dynamic indexes of gas emission”, *Disas. Adv.*, **3**(4), 403-406.
- Yang, Z. and Zhou, S. (2015), “Modeling and prediction of daily gas concentration variation at a mining face based on the elliptic orbit model: A case study”, *J. Min. Sci. Technol.*, **25**(6), 1045-1052.
- Yu, B., Su, C. and Wang, D. (2015), “Study of the features of outburst caused by rock cross-cut coal uncovering and the law of gas dilatation energy release”, *J. Min. Sci. Technol.*, **25**(3), 453-458.
- Zhou, F., Sun, Y., Li, H. and Yu, G. (2016), “Research on the theoretical model and engineering technology of the coal seam gas drainage hole sealing”, *J. Chin. U. Min. Technol.*, **45**(3), 433-439.
- Zhang, R. and Ian, S.L. (2010), “The application of a coupled artificial neural network and fault tree analysis model to predict coal and gas outburst”, *J. Coal Geol.*, **84**(2), 141-152.
- Zhang, T., Ren, S., Li, S., Zhang, T. and Xu, H. (2009), “Application of the catastrophe progression method in predicting coal and gas outburst”, *Min. Sci. Technol.*, **19**(4), 430-434.